JGR Biogeosciences

RESEARCH ARTICLE
10.1029/2019JG005395

Vegetation Trajectories and Shortwave Radiative Forcing Following Boreal Forest Disturbance in Eastern Siberia

S. M. Stuenzi[1,2,3] and **G. Schaepman-Strub**[1]

[1]Department of Evolutionary Biology and Environmental Studies, University of Zurich, Zurich, Switzerland, [2]Alfred Wegener Institute Helmholtz Centre for Polar and Marine Research, Potsdam, Germany, [3]Geography Department, Humboldt University of Berlin, Berlin, Germany

Key Points:
- Major boreal forest cover disturbance in the coldest region of the Northern Hemisphere (Yakutsk, Siberia) during 2001–2014 resulted in a significant change in surface albedo
- Surface albedo change-related mean annual surface shortwave radiative forcing was −6.015 W/m^2 but varied with season and strongly decreased during the 13 years following disturbance
- Shortwave radiative forcing can be directly linked to a vegetation trajectory from deciduous needleleaf to broadleaf dominated forest

Supporting Information:
- Supporting Information S1

Correspondence to:
S. M. Stuenzi and G. Schaepman-Strub,
simone.stuenzi@awi.de;
gabriela.schaepman@ieu.uzh.ch

Citation:
Stuenzi, S. M., & Schaepman-Strub, G. (2020). Vegetation trajectories and shortwave radiative forcing following boreal forest disturbance in eastern Siberia. *Journal of Geophysical Research: Biogeosciences*, *125*, e2019JG005395. https://10.5194/10.1029/2019JG005395

Received 25 JUL 2019
Accepted 15 APR 2020
Accepted article online 23 APR 2020

Author Contributions:
Conceptualization: S. M. Stuenzi, G. Schaepman-Strub
Funding acquisition: S. M. Stuenzi, G. Schaepman-Strub
Methodology: S. M. Stuenzi, G. Schaepman-Strub
Project administration: S. M. Stuenzi, G. Schaepman-Strub
Supervision: G. Schaepman-Strub
Writing - original draft: S. M. Stuenzi, G. Schaepman-Strub
(continued)

Abstract Major boreal forest disturbance and associated carbon emissions have been reported in the coldest region of the Northern Hemisphere. Related biophysical feedbacks to climate remain highly uncertain but might reduce warming effects expected from carbon emissions. This study quantifies albedo change after disturbance, primarily fires, in larch-dominated forests around Yakutsk as compared to undisturbed areas with natural albedo variability, using satellite-based time series. The related annual mean shortwave radiative forcing was −6.015 W/m^2 for the 13 years following forest disturbance. It was highly negative during snow-covered months (−3.738 to −13.638 W/m^2), but positive (+5.441 W/m^2) for the summer months in the first year after disturbance, decreasing afterward and also turning into a negative forcing after 5 years. Forcing by surface shortwave radiation must be considered to assess the impact of boreal forest disturbance on climate and additional feedbacks, such as increased permafrost thaw or transition to alternative ecosystem states.

Plain Language Summary Boreal forests of northeastern Siberia are experiencing disturbances such as fires and permafrost degradation. These disturbances can trigger changes in biomass and heating dynamics resulting in major feedbacks to the local and regional climate. This study quantifies albedo, the ratio of reflected sunlight to incoming sunlight, in a larch-dominated forest area in Siberia over a time span of 13 years after fire disturbance. Land surface albedo showed significant changes due to larch forest disturbance, which often recovered to a birch-dominated forest. During summer months of the first 4 years after the forest fire, the decrease in albedo caused a local warming. For snow-covered seasons, forest disturbance and the corresponding albedo change caused low local cooling directly after disturbance, and this cooling effect increased during the following decade.

1. Introduction

Boreal forests cover more than 30% of the total forest area of the terrestrial Earth surface and are claimed to form one of the last intact biomes with 44% undisturbed and isolated from anthropogenic influences (Brandt et al., 2013). Due to their extent, they store twice as much carbon as tropical forests. However, with changing natural regimes, logging and primarily human-caused fires large amounts of carbon, accumulated over centuries, could be released (Achard et al., 2006). In addition to these biogeochemical feedbacks, boreal forest disturbance impacts climate through altering biophysical interactions (Bonan, 2008; Duveiller et al., 2018; Snyder et al., 2004), but the amount of related studies is much lower than for other forcings (Bonan et al., 1992; Myhre et al., 2013). Disturbance of boreal forest was reported to increase surface albedo, reduce net radiation and surface temperature, and precipitation (Bala et al., 2007; Li et al., 2015; Z. Liu et al., 2019; Snyder et al., 2004), but the net climate effect depends on the forest structure and climate conditions (Shuman et al., 2011). A complex canopy has a low albedo due to its higher efficiency in capturing light (Baldocchi et al., 2004; Dickinson et al., 1993). Climate forcing from an increasing albedo could offset the forcing induced by carbon emissions through forest disturbance (Bonan, 2008).

Boreal forests of Eastern Siberia are located between 50°–66°N and 94°–140°E covering an area of 1.93 × 10^8 ha underlain by continuous permafrost. They differ from other boreal forests because they are dominated by larch (*Larix*), a deciduous genus. This has implications on the nutrient cycling as well as the albedo (Chen et al., 2016) and the fire cycle. In North American boreal forests, most fires are high-intensity crown fires, which combust large amounts of vegetation and release black carbon aerosols that accelerate snow and

Writing – review & editing: S. M. Stuenzi, G. Schaepman-Strub

ice melt. High-intensity fires lead to a replacement of the forest and a new successional sequence (De Groot et al., 2013). In the Siberian taiga, low-intensity surface fires are more common (Ponomarev et al., 2016). They favor the selection of fire-tolerant trees such as pine and larch and can occur many times within the life of a forest stand. Nevertheless, and despite the substantial gain in boreal forests globally and in Russia, Russia has the highest total loss of forest area in the world and also a high net loss (Hansen et al., 2013). A high correlation between forest change (Hansen et al., 2013) and Moderate Resolution Imaging Spectroradiometer (MODIS) active fire data (Giglio et al., 2003) suggests that forest fires are the main reason for extensive forest loss and forest transitions reported in Siberia. Unfortunately, the fire record is poorly documented. Annually, 200–1,400 fires occur in the Sakha republic. A rough estimate of 15–30% is caused by lightning, the rest by humans. The total burned area accounted for 115,400 km^2 between 1955 and 2002 (Hayasaka, 2002). The needle shedding of the larch trees produces a very flammable layer on the forest ground. The number of forest fires and the size of the burned area in Eastern Siberia has increased strongly over the past decades, supporting the hypothesis of climate-driven increase in forest fire frequency (Ponomarev et al., 2016). Most forest fires in the study area are recorded in the hottest months June (28%) and July (58%), while 6% occur in May and 16% in August (Valendik, 1996). They take place early in the fire season when big amounts of dry, dead surface fuel have accumulated and the forests can quickly catch fire, usually through anthropogenic interferences (Ivanova, 1996). Later in summer, the understory plants green up, and lightning becomes the dominant cause of fire (Shvidenko & Nilsson, 2000). Forests around Yakutia burn every 15–20 years (Prof. Dr. A. Isaev, personal communication, 6 July 2017). The average dieback period is estimated to be 5 years, and increased tree mortality is observed for up to 10 years after a fire (Takahashi, 2006). Postfire regeneration depends on many factors such as climate and geographic distribution, landscape structure and relief, biological and ecological properties of the species, forest type and succession stage, availability of seeds, and type of fire regime (Otoda et al., 2013; Takahashi, 2006). New thermal conditions, additional soil drainage or higher soil wetness, enrichment in nutrients after a fire, and an increased active layer depth can all have a favoring effect on either pine or birch expansion on the cost of larch-dominated forest (Liu et al., 2017; Takahashi, 2006). Soil moisture and precipitation are the limiting factors for larch growth (Rogers et al., 2015). The white birch regenerates well after fires and is not dependent on nearby seed sources (Rogers et al., 2015).

Climate warming is predicted to impact vegetation composition directly as well as indirectly through permafrost thaw and forest fires (Beer et al., 2007; Boike et al., 2016; Forkel et al., 2012; Tchebakova et al., 2009). Namely, the lengthening of the fire season could influence and fasten the transition of larch-dominated forests toward steppe or grasslands (Gauthier et al., 2015; Otoda et al., 2013; Tchebakova et al., 2009). In field observations in Siberian larch forests, Kharuk et al. (2007) found a spreading of evergreen coniferous (spruce and fir) and broadleaf (mostly birch) forests that are more tolerant to higher temperatures. They further found that burned forest patches can serve as ecological niches for the establishement of evergreen conifers and deciduous broadleafs. In their study, the pine and birch undergrowth was more abundant at former fire sites (Kharuk et al., 2005; Kharuk et al., 2007). Chu et al. (2017) study on a larch (*Larix sibircia*) forest in Siberia showed that high-severity burns are the preferable condition for a fast spreading of shrubs, grasses, and broadleaf trees, while moderate-burn severity shows a high rate of larch recruitment. They conclude that severely burned larch forests will require a long recovery period and possibly never fully recover to their previous net primary productivity due to the dominance of broadleaf trees.

Current literature highlights large uncertainties in albedo and related radiative forcing in the boreal biome. The latest IPCC report predicts a negative forcing of −0.2 W/m2 by deforestation through increased land-surface albedo, with the largest contribution by high-latitude forests (IPCC, 2014; Myhre et al., 2013). The uncertainty of this estimate is 0.2 W/m^2, and the level of scientific understanding is lower than for the other radiative forcing components (IPCC, 2014). Deciduous tree species such as birch have a higher albedo than evergreen stands, in summer, but especially in winter (Kuusinen et al., 2014). In summer, larch albedo is approximately 0.133, birch 0.152, and evergreen around 0.079 (Hollinger et al., 2010). Siberian forests have a strong warming effect, covering highly reflective snow that is present most of the year (Bala et al., 2007; Bonan, 2008; Shuman et al., 2011). Several studies concluded that deforestation in boreal areas would lead to local cooling (Bonan et al., 1995; Otterman et al., 1984; Thomas & Rowntree, 1992). Even when taking the warming effect by decreased carbon sequestration into account, a reduction of boreal forest would still cool the climate (Bala et al., 2007; Bathiany et al., 2010; Betts, 2000). O'Halloran et al. (2011) found that

climate forcing due to the albedo change associated with natural disturbances such as hurricanes, wildfires, or beetle infestation was in the same order of magnitude as the CO_2 forcing. Where snow was present, removal of the vegetation or foliage created a cooling feedback. Liu et al. (2019) showed that fire-induced forest losses accounts for about 15% of global forest loss, of which most occurs in high latitudes. They found an initial warming of the surface temperature by 0.15 K 1 year following fire in burned area globally. In high latitudes this positive feedback was mainly caused by reduced evapotranspiration and sustained for about 5 years. Long term, the increases in albedo dominated the surface radiative budget resulting in a net cooling effect (Liu et al., 2019). Lyons et al. (2008) analyzed the shortwave surface forcing through forest loss in interior Alaska. They found an average forcing of -6.2 W/m^2 for the first five decades relative to an undisturbed coniferous control and -3.0 W/m^2 relative to a control reconstructed from preburn observations. In a similar study, Randerson et al. (2006) constructed a radiative forcing trajectory for disturbed black spruce forests in interior Alaska and found a negative forcing which lasted for 50 years. A further study in burned forests of North America found the same magnitude of surface forcing (-5 to -8 W/m^2) through albedo change (Rogers et al., 2015). In a recent study, Chen et al. (2018) quantified the surface radiative forcing of stand-replacing forest fires in Siberian larch forests, and their results are in line with a strong overall cooling effect caused by an increase in surface albedo in snow-covered periods.

This study aims at quantifying the surface shortwave radiative forcing through surface albedo changes by assessing the postfire vegetation trajectories in boreal forests in Eastern Siberia where extensive forest disturbance has been reported. Based on a comparison of potential land surface trajectories and related uncertainties of radiative forcing, we complement previous modeling studies of forest disturbance effects on albedo and shortwave radiation forcing. We used satellite-based albedo time series over 13 years to observationally determine seasonal and annual albedo and shortwave radiation forcing trajectories.

2. Material and Methods

We combined Landsat-based forest change data by Hansen et al. (2013), MODIS broadband albedo, and in situ irradiance data to assess postfire albedo changes and the resulting surface shortwave radiative forcing. All analyses were performed using Google Earth Engine (Gorelick et al., 2017), ArcMap 10.4.1 (ESRI, 2011), and RStudio 3.3.1 (R Core Team, 2016).

2.1. Study Area

The study area is located west of Yakutsk (121.9–128.2°E, 61.3–63.6°N) and has a total size of 180,000 km^2 (Figure 1). The forests are dominated by *Dahurian* larch with understory vegetation such as *Vaccinium vitis-idaea*, which occupies 89–90% of the forested area. Another 6% is covered by scots pine (*Pinus sylvestris*) on dryer and sandier soils. The rest of the area is vegetated by willow birch, an early successor after forest disturbances. The larch forest stand density is 840 trees ha^{-1}, and mean stand height is 18 m (Ohta et al., 2001).

The climate in the Siberian taiga can reach extreme temperatures of -62°C in winter and up to 35°C between May and September. The annual average temperature is below 0°C and results in continuous permafrost and therefore poorly drained, podzolized, and nutrient-poor soils (Chapin et al., 2011). Our analysis of monthly surface temperature using Climatic Research Unit TS4.01 data (Harris et al., 2014) shows a positive temperature trend from 1970 to 2010 for spring, summer, and fall (Figure 2a) and a negative trend for winter. The fire season precipitation has decreased over the past 30 years (Hayasaka, 2002). However, the burned area does not show a significant trend for the study area nor for the larger region (115–140°E, 55–75°N), for the period 1997 to 2016, based on our analysis of the Global Fire Emissions Database Version 4.1 with small fires (GFED4.1 s) (Randerson et al., 2012) (Figure 2b). Nevertheless, exceptionally large burned areas were recorded in 2002 and 2014 for the study area, while the larger region in addition showed extensive burned areas in 2012 (Figure 1).

2.2. Satellite-Derived Land Surface Albedo

Albedo trajectories were derived based on the MODIS white-sky (bihemispherical reflectance) shortwave broadband albedo product (MCD43A3 Version 6; Schaaf & Wang, 2015), as available in Google Earth Engine for the years 2001–2014. The MCD43A3 product is generated daily, using a 16-day composite retrieval algorithm and uses an improved back up database with pixel-based updates from the latest full inversion as compared to earlier versions. Further, there is improved quality at high latitudes because all available

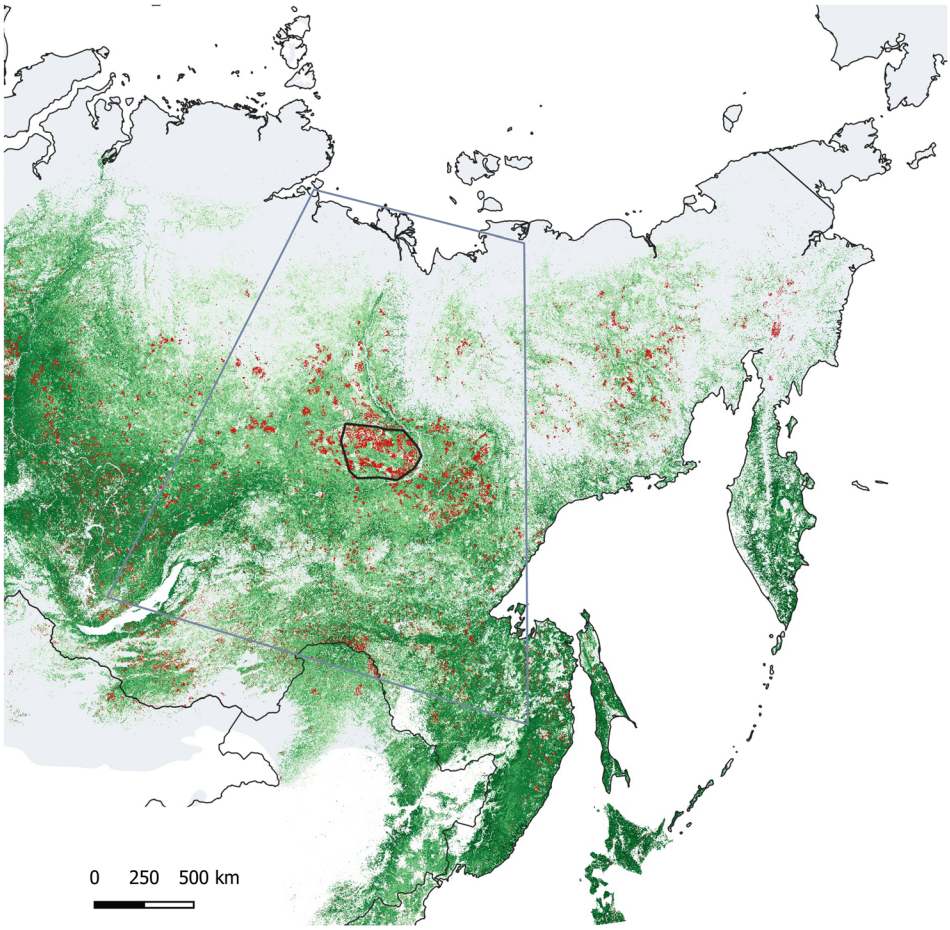

Figure 1. Map of forest cover in 2000 (green) (data source: Hansen et al., 2013), permafrost extent (gray) (data source: Brown et al., 2002) and forest disturbance from 2000–2014 (red) in eastern Siberia (data source: Hansen et al., 2013). The smaller black polygon shows the study area, and the gray polygon is the larger region.

observations are used (for further information see Schaaf & Wang, 2015). Detailed validation data over boreal forest areas are not available yet for product Version 6. For Version 5, the root mean square error (RMSE) of the full inversion albedo data over needleleaf forest was 0.014, over broadleaf forest 0.02, and over mixed forest 0.014 (Wang et al., 2014). A difference in albedo smaller than 0.014 is therefore within

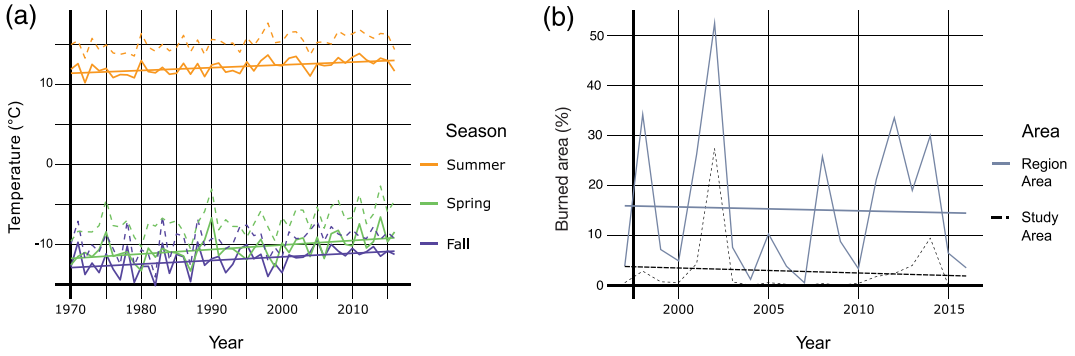

Figure 2. (a) Temperature trends for fall, spring, and summer seasons, displayed for the study area (dotted lines) and the larger region (solid lines) (data source: Climatic Research Unit (CRU) TS4.01 data (Harris et al., 2014)). (b) The burned area trend for the study area and the region (source: Global fire emissions database version 4.1 with small fires [GFED4.1s]; Randerson et al., 2012).

the uncertainty of the albedo data and does not necessarily represent changing surface properties. There are no available observations for December, due to the unavailability of high-quality data because of the large solar zenith angles at high latitudes (Lyons et al., 2008).

2.3. In Situ Incoming Shortwave Radiation Data

At the Spasskaya Pad research station (https://eu-interact.org/field-sites/spasskaya-pad-scientific-forest--station/) inside the chosen study area, micrometeorological variables are measured on two observational towers since 1996. The frequency of measurements is 30 min, resulting in 48 measurements per day for the 2003–2007 time period (AsiaFlux, 2017; Maximov, 2015). The mean monthly incoming shortwave radiation data of 2005, measured above the tree canopy, at a height of 32 m above the ground, are utilized as a representative proxy for the region to calculate the surface shortwave radiative forcing.

2.4. Surface Shortwave Radiative Forcing

Radiative forcing is a concept to estimate the impact of a perturbation on the radiative energy budget of the Earth system (IPCC, 2014). The forcing results from changes in the incident solar radiation, and radiatively active atmospheric components, such as CO_2 and aerosols. Changes in land surface albedo have a high potential for climate forcing (J. Hansen et al., 1993, 1997). We use the surface shortwave radiative forcing (W/m^2) to describe a potential warming or cooling effect of forest change on climate.

$$SSRF = \alpha^{*}K_{in} \tag{1}$$

Equation 1 describes the surface shortwave radiative forcing (SSRF) as the change in albedo (α) multiplied by the incoming shortwave radiation (K_{in}) (Jiao et al., 2017).

2.5. Spatial Sampling Design and Analysis

Hansen et al.'s global forest change data were used to determine the year of forest loss between 2001 and 2014 (Figure S1 in the supporting information). The definition of forest loss as used in Hansen et al. (2013) was adopted referring to "a stand-replacement disturbance or the complete removal of tree cover canopy at the Landsat pixel scale" (Hansen et al., 2013). According to this definition, forest loss is not necessarily permanent, and the disturbed forest might recover or remain treeless and transition toward a different land cover class.

According to the year of forest loss detection (2001–2014), the study area was divided into 13 classes of recovery age after loss detection (R1 containing all areas 1 year after loss detection to R13 containing all areas 13 years after loss detection). The area, where no forest loss was detected, served as control (C) and was randomly subsampled to the median size of the loss areas (2,738 km^2) across all years for statistically balanced comparison. Areas occupied by lakes and roads (2.4%), nonforest vegetation or forest loss followed by gain (44%), were excluded from this study. The spatially averaged monthly albedo (see section 2.2) of every loss and control area was exported from Google Earth Engine. The following statistical analyses were implemented in the R environment Version 3.3.1 (R Core Team, 2016) to determine the seasonal albedo and surface shortwave radiative forcing trends in the study area. The monthly albedo values of the loss areas were averaged per season (spring [March–May], summer [June–August], fall [September–November], and winter [December–February]), by recovery age to analyze the postfire trajectory (Figure S2). Finally, the values for each recovery area over the whole period were grouped by recovery age, and the surface shortwave radiative forcing ($SSRF_{R1–13}$) was calculated for each month (equation 2), using the shortwave irradiance (K_{in}) and the albedo difference ($\Delta\alpha$) between the forest loss area albedo for each recovery age ($\alpha_{R1–13}$) and undisturbed, control forest albedo (α_C).

$$SSRF_{(R1–13)} = (\alpha_C - \alpha_{R1–13})^{*}K_{in} \tag{2}$$

Monthly SSRF values were then also averaged to seasonal and annual values of forcing.

In a second approach we analyzed how the albedo is affected if deciduous needleleaf changes to a broadleaf dominated forest, based on land cover type data (MODIS MCD12Q1.006) available in Google Earth Engine at yearly intervals with a spatial resolution of 500 m. We subsampled an area with a total size of 490 km^2, dominated by decidous needleleaf forest and located around the Spasskaya Pad research station at 62°14′

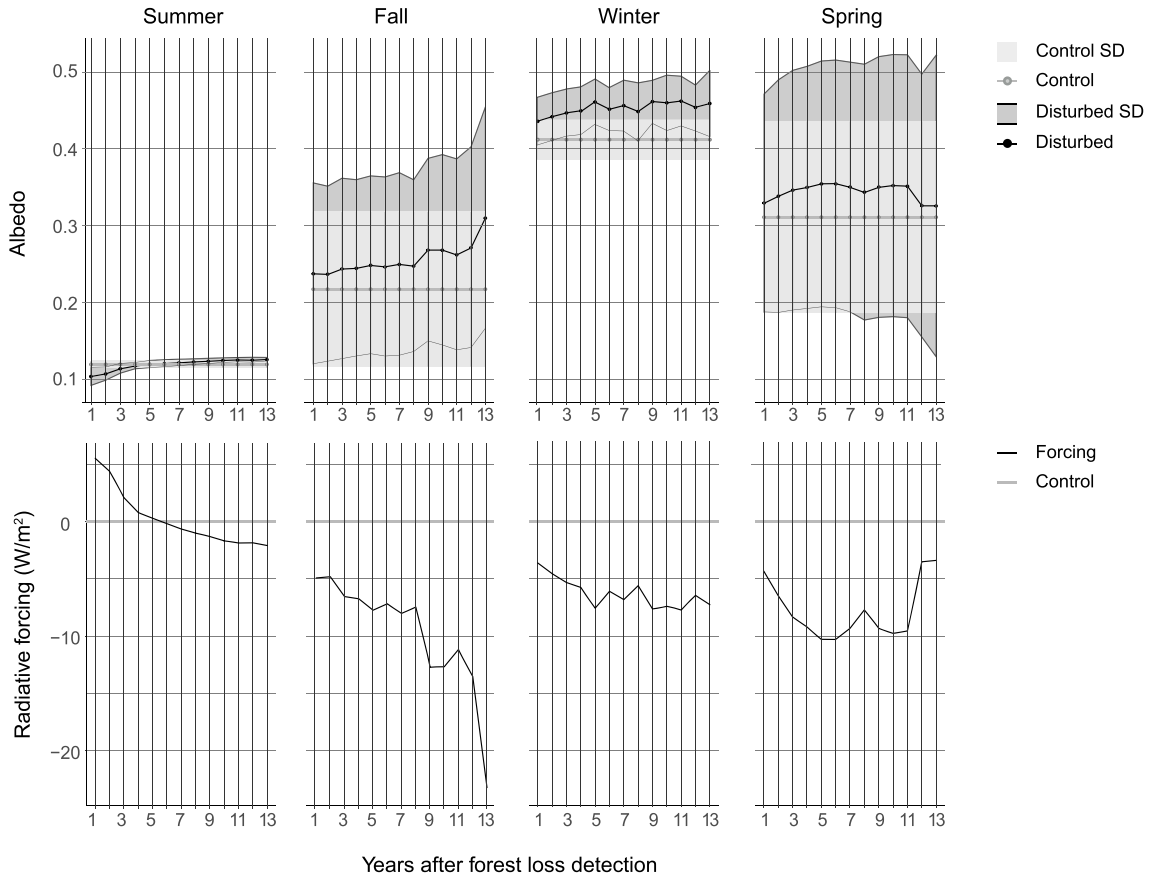

Figure 3. Top: mean seasonal albedo of the control areas (gray, with spatial standard deviation) and of the loss areas (black) with standard deviation (light gray). Bottom: the resulting surface shortwave radiative forcing (W/m^2) of the loss area, in relation to the control area, for 13 years following forest disturbance.

N, 129°37′E. Part of this forest, an area of 224.9 km^2, was disturbed in the very high intensity fires of 2002 and showed a trajectory toward broadleaf-dominated forest afterward, based on our analysis of landcover type data of 2004–2014. The monthly mean albedo of these deciduous needleleaf and broadleaf dominated areas was exported and compared for to understand the impact of vegetation-type trajectories after forest loss and related seasonal and monthly albedo and respective radiative forcing trends.

3. Results

In total, over 53% of the study area and 60,995.9 km^2 of land experienced forest disturbance in the years 2001–2014 (Figures 1 and S1). The highest forest loss was detected in 2002–2004, with 18,000 km^2 in 2003 alone (for further information see Text S3).

We have found pronounced effects of disturbance on albedo with high seasonal variability. An albedo change was detected in all areas following forest disturbance (Figure 3 and Table S4). Additionally, to quantify the albedo of undisturbed forests and its natural variability, we assessed the albedo mean and temporal variance of control areas. The albedo variation observed in different years was lower in the control areas than in the loss areas. Average control albedo for winter is 0.423 (±0.013). Winter albedo was higher after the forest loss event in all affected areas. It increased for 7 years and then stabilized at 0.03 above the control. The mean winter albedo in the loss areas was 0.453 (±0.033). Average spring albedo in the control areas is 0.311 (±0.041). In spring, mean albedo of all loss areas was higher than the control with 0.344 (±0.164). It increased during the first 5 years, stabilized for another 6 years and dropped to a value only slightly higher than the control. Average summer albedo in the control areas is 0.120 (±0.005). Summer albedo 1 year after the forest loss was 0.104 (±0.012) and stayed lower in the first 5 years after the loss event and then increased above the control. The mean summer albedo across the loss areas was 0.119 (±0.005). Average control albedo

for fall is 0.218 (±0.025). The mean fall albedo was also higher than the control with 0.257 (±0.121), with a steady increase toward the end of the study period, with no stabilization even 13 years after disturbance.

Based on the change in albedo, an overall negative forcing and some positive summer forcing were found. The average annual forcing for the first 5 years was −4.28 W/m^2, increasing to −6.015 W/m^2 when considering the first 13 years (maximum time span covered in this study) after forest disturbance. The highest negative forcing was found in spring 5 years after forest loss detection (−10.4 W/m^2) and in fall, between 9 and 12 years (−13.6 to −11.3 W/m^2) and after 13 years (−23.3 W/m^2), possibly due to early snowfall. The standard deviation is generally lowest during winter months (with a minimum of ±0.35 in winter season of Year 12) and during summer and winter months of the first recovery years and increases toward later succession stages, especially during spring, summer, and fall months in Years 11–13 (with highest standard deviation in summer season of year 12 with ±59.06). In winter, the shortwave surface radiative forcing was between −3.7 W/m^2 (after 1 year) and −7.8 W/m^2 (after 11 years) (Table S5 and Figure 3). The results show a warming effect in the summer months with a maximum in the first year after forest loss detection (5.44 W/m^2), with a decreasing trend, finally switching to a cooling effect, 6 years after disturbance. The magnitude of the summer warming of the first 5 years is of a different magnitude compared to the negative forcing of the other seasons and the late summer forcing (see Table S5). The total positive forcing sums up to 12.451 W/m^2, the total negative forcing across all seasons and all years to −325.863 W/m^2. The negative forcing is stronger by a factor of 26.

Our second analysis provides insight into albedo trajectories of specific forest-type patches over time. The areas of deciduous needleleaf forest with trajectories to broadleaf-dominated forests after disturbance in 2003 and 2004 showed a mean annual albedo of 0.272 (±0.032), while the undisturbed deciduous needleleaf (larch) forests had a mean annual albedo of 0.205 (±0.036). Mean winter albedo for broadleaf was 0.377 (±0.075) and for deciduous needleleaf 0.474 (±0.040), while mean summer albedo was 0.114 (±0.012) for broadleaf and 0.112 (±0.008) for deciduous needleleaf. Winter and spring albedo for the disturbed areas increases until year 2013. Summer albedo increases for 7 years and then stabilizes with a slight decrease toward Year 2014, and fall follows no clear trend. These trends from 2004–2014 are visible in Figure 4.

Based on the change in albedo resulting from transition of deciduous needleleaf to broadleaf forest, we calculated the radiative forcing. An average forcing of −13.68 W/m^2 occurred for the first 5 years, increasing to −15.42 W/m^2 when considering the first 10 years (maximum time span covered in this study) after forest disturbance. The highest negative forcing was found in spring 9 years after forest loss detection (−52.98 W/m2). In winter, the shortwave surface radiative forcing was between −1.87 W/m^2 (after 5 years) and −29.26 W/m^2 (after 9 years).

4. Discussion

While analyzing forest loss in our study area, we detected a time lag in Hansen's global forest change data. According to local researchers and media coverage the biggest fires around Yakutsk occurred in 2012 and 2002, affecting 2 and 1.5 million hectares, respectively. Additionally, 2008 and 2011 were very fire intensive years. Based on this knowledge and according to Oleg A. Tomshin (personal communication, 5 July 2017), the peak in 2003 in forest loss detected in our study area based on Hansen's global forest change data was not explicable. To investigate this further, the MODIS active fire data were visualized for comparison with the forest change data (Figure S3). A high spatial correlation between the two data sets is visible. The temporal correlation however is low. This is especially apparent during the intense fire years of 2002 and 2011, for which part of the disturbed areas are detected as forest loss in the years 2003 and 2012. This time lag indicates that the algorithm of the forest change data does not detect all the loss indicated by the MODIS active fire data. Some of the loss areas are detected in the following year only, implying various issues for using the forest change data. To better understand the underlying problem, we analyzed the data at monthly time scale. The months with the highest proneness to missing detection are August and September, 2 months dominated by strong, stand-replacing fires (see Text S3). The potential time lag in detection for part of the loss areas indicates that albedo values might not all be assigned to the actual year of forest loss but that recovery age classes might integrate values over 2 years instead of 1 year only. While the overall trajectory in resulting forcing is expected to be maintained, the absolute values might be smoothed out by integration across two recovery age classes due to the time lag in detection.

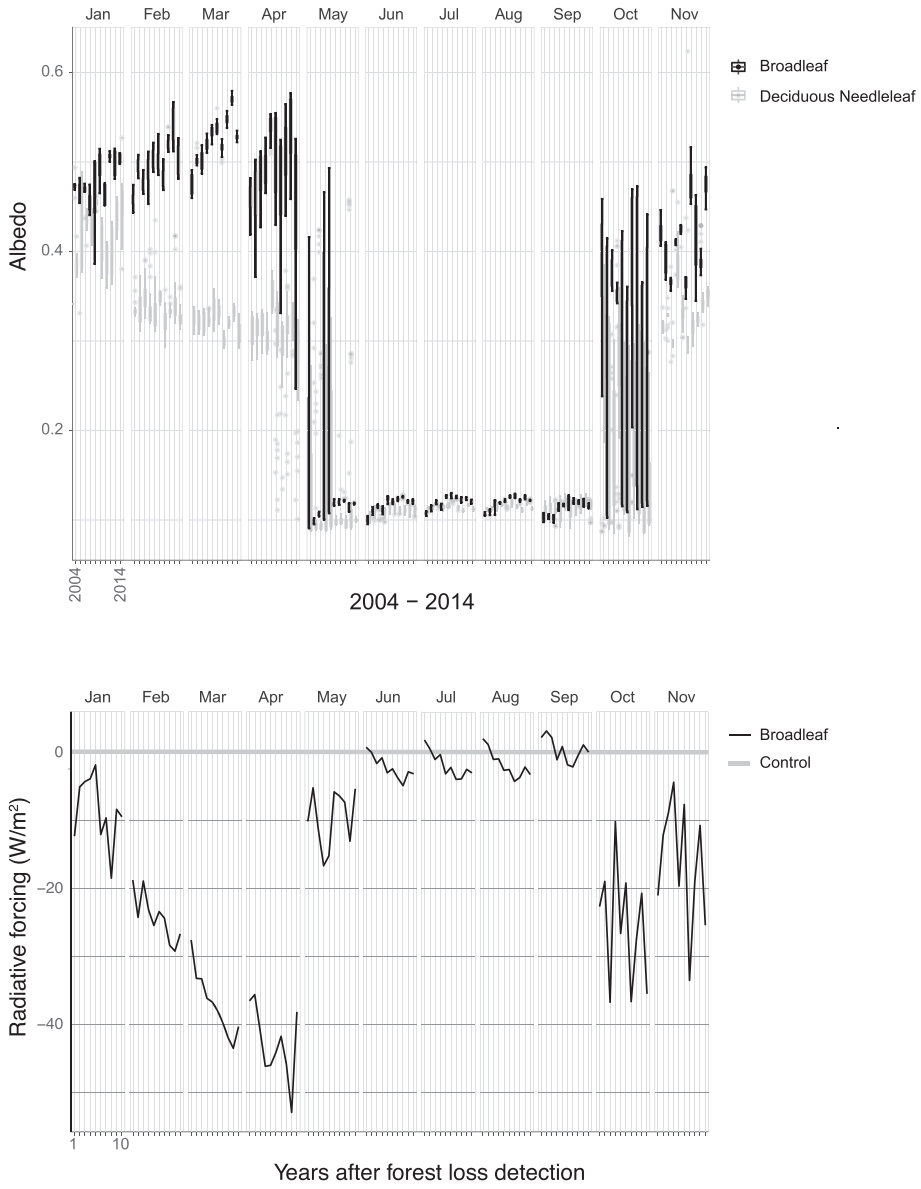

Figure 4. Albedo trajectory from January to November in deciduous needleleaf (light gray) and broadleaf (dark gray) dominated forest stands with the standard deviation. For each month, albedo trajectories through 11 years (2004–2014) are displayed.

The differences in albedo values between the seasons are high and are only partly due to forest change. Spring and fall have a high albedo variance due to snowmelt and snowfall (Figure 3). Therefore, the albedo trajectories for these seasons should be interpreted with caution, even though a higher mean spring and fall albedo were found for all disturbed compared to undisturbed forests. Additionally, the trends in the albedo trajectories of recovering areas are not adequately displayed by the means, because they are then evened out. This is especially relevant to the average summer albedo, which is barely lower than the average of the control, because of the displayed trend from a positive to a negative forcing. While summer albedo changes are low compared to winter changes, irradiance levels are much higher, leading to a considerable summer radiative forcing. In fall of the 13th recovery year, the strongest negative radiative forcing was observed. However, this value is based on a single year of forest loss, that is, 2001, and could therefore be biased toward the specific fire severity of 2001 as compared to more balanced samples across several years. These areas are the only ones that could reach 13 years of recovery in this study setup.

Average summer forcing over control areas observed in this study (-6.027 W/m^2) is very similar to the forcing (-6.2 W/m^2) to a coniferous control and averaged over the first five decades simulated by Lyons et al. (2008), despite the difference in geographic range. This suggests similar driving factors in different boreal forest zones. The study by Lyons et al. was conducted over a large and very heterogeneous study area of 446,000 km^2, including not only forested areas, like evergreen needleleaf forest (10,6%, IGBP classification) but also open shrubland (25%) with relatively low density stands of black spruce and therefore little dense forest canopy. Tundra and shrub-dominated areas are expected to show a much smaller response in albedo difference after fire disturbance because in the absence of a canopy overstory, winter albedo change will be much smaller. Therefore, the homogeneous area considered in this study is expected to show a clearer signal. With this in mind, this study's found estimate of -6.027 W/m^2 supports the growing body of work concerning the surface shortwave radiative forcing of boreal forest loss (e.g., Chen & Loboda, 2018; Chen et al., 2018). The advantages in this study are the use of daily MODIS Version 6 albedo and land cover data, the local irradiance data, and the local and very stable control areas as well as the higher seasonal resolution of the albedo and radiative forcing results.

We show that areas originally dominated by deciduous needleleaf forest and following a trajectory to broadleaf forest after stand-replacing fires of 2003 and 2004 do neither recover to larch dominated forests in the studied time period nor reach predisturbance albedo values through an equally dense canopy closure (Figures 4 and 5). This is especially visible in the statistically significantly different albedo values of February, March, and April. During these snow-covered months, the disturbed areas have a differing albedo across the whole study period. The increasing albedo in the winter, spring, and fall seasons found in this study can be interpreted as an indicator for a temporary succession toward a less complex ecosystem structure or open ground (as shown in Figure 5). Even though most of the fires in the study area were expected to be of low intensity, the loss areas of 2002, 2003, 2008, 2011, and 2012 seem completely disturbed based on the very profound albedo changes. Even if most trees are still standing as snags or if wood is laying on the ground, the less-disturbed snow cover on the forest ground (compared to a snow-covered canopy) and less shading of the snow-covered ground would lead to pronounced albedo differences. The negative summer shortwave radiative forcing after 6 years indicates a succession toward either broadleaf forests composed of lighter birch trees (Hovi et al., 2016), young larch or pine saplings or shrubs and grasses with a higher summer albedo than the previous larch forests or wetlands (Lyons et al., 2008; Randerson et al., 2006). This is comparable to the postfire trajectories in North American boreal forests, where deciduous broadleaf species dominate in the early successional stages (Lyons et al., 2008). In agreement with the latest study by Chen et al. (2018), we propose that these stand-replacing fires have a considerable effect on the overall surface radiative forcing trajectory of all disturbance areas combined. As visible in Figure 4, the lower summer albedo in the first 5 years after a fire disturbance is not as pronounced in areas with a trajectory toward broadleaf forests, suggesting that birch and broadleaf bushes are fast successors and quickly cover char (Chen et al., 2018) and dead wood depositions. The positive summer forcing must therefore mainly result from the effects of the nonstand-replacing fires on the larch stands, such as the darkening of the forest ground and the removing of parts of the canopy.

Changes of the surface properties are especially crucial in the boreal forest eco-zone because of the underlying permafrost and its potential of thawing and transforming into a carbon dioxide or methane source. Wildfires affect the permafrost mostly because of removal of the vegetation, which reduces evapotranspiration and increases the soil moisture content. Soil moisture, temperature, and the density of the organic layer influence the thermal conductivity and determine whether the active layer is deepening after a wildfire (Yoshikawa et al., 2002). If the organic layer is thick enough, the active layer will not be depressed, and the only immediate change remains the lower summer surface albedo. In the cold season, less vegetation cover leads to an even snow layer with a very high albedo, resulting in a negative surface shortwave radiative forcing and less heat absorption. At a larger scale, this might contribute to a local cooling, which opposes the positive forcing resulting from the other, mainly biochemical effects of the forest disturbance (i.e., Bala et al., 2007; Duveiller et al., 2018). In terms of the surface shortwave radiative forcing, there is an overall local cooling effect if boreal forests are lost, due to the higher albedo in nine out of 12 months. Nevertheless, the forcing is positive in the warm summer months of the first years, and the surfaces have been altered drastically, especially in recent and very destructive fires. In the summer months of the first 4-year past disturbance, the altered vegetation cover leads to a lower albedo, a positive surface shortwave radiative forcing

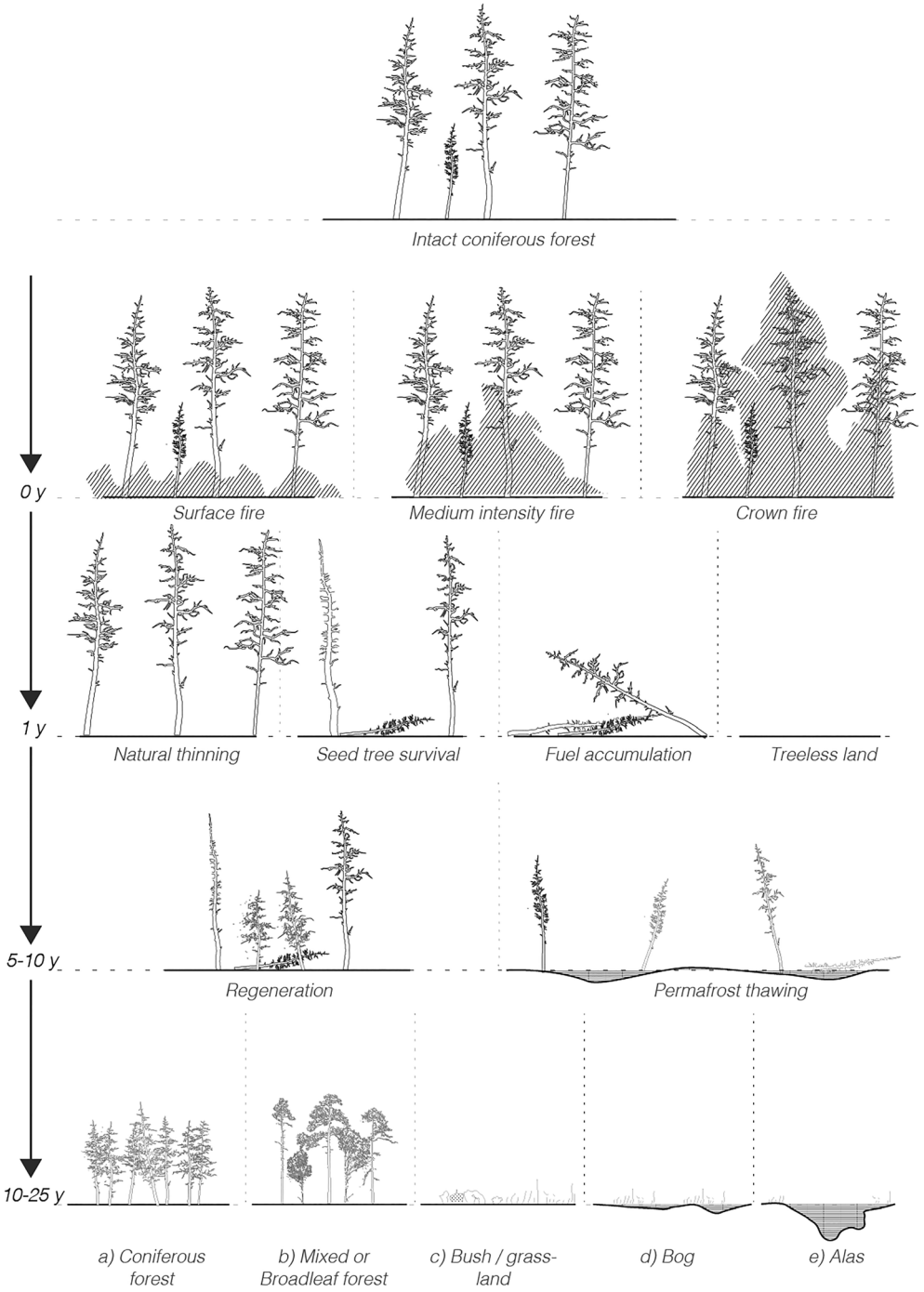

Figure 5. Land-surface trajectories after forest fires. Natural thinning describes the death of young or previously damaged trees, developing into a healthier, quickly recovering forest. If seed trees survive, a recovery of the needleleaf forest is likely despite the death of most trees. Fuel accumulation represents the mortality of all trees resulting in a lot of burned material, adding to the biomass available for regrowth and recuperation. A treeless land surface remains after a very intense crown fire, which leaves nothing but ashes. Dependent on these scenarios the area can either recover into (a) a coniferous forest of the previous or a differing composition, (b) mixed or broadleaf-dominated forest, (c) bushland or grassland, (d) bog, or (e) an alas, with respective trends in surface conditions and alterations in surface albedo (modified after Takahashi, 2006).

and less isolation of the ground which results in a higher energy absorption, a local warming and an enhancement of the other positive forcing caused by the forest disturbance. The severity of the disturbance determines the duration of these warming effects. Further, the positive summer forcing will become more important with extended summers and shorter and drier winters under observed and expected climate warming. The cooling effect of winter might also decrease if drier and warmer winters result in less or no snow in a future climate.

The future importance of the shortwave radiation forcing through fire disturbance will depend on how the fire frequency, severity, and burned area will develop. Origins of fires are not well documented in the literature for the Sakha Repulic, Yakutia. It remains unclear how large the anthropogenic versus natural ignition contributions are, and if these have changed with sociopolitical transitions and climate change in the area. Extremely warm and dry springs and early summers, as experienced in 2019, will certainly favor spreading of fires. Once ignited, fires are left to spread naturally as the forests around Yakutsk have been labeled as "distant and hard-to-reach territory," and the current law and regulations do not enforce fire control as long as cities or settlements are not directly affected. Increasing the knowledge on the origins of fires is therefore a prerequisite for predictions of forest disturbance and related radiative forcing through albedo change.

5. Conclusion

A changing albedo due to forest disturbance can either enhance or weaken the forcing caused by the release of greenhouse gases through decrease of biomass, CO_2 sequestration and evapotranspiration, and permafrost thaw. In all areas, the surface shortwave radiative forcing showed a sharp response to forest disturbance for the analyzed time periods of up to 13 years. Even though forest disturbances resulted in a negative shortwave radiative forcing effect, they could trigger other effects with positive climate forcing, mainly the thawing of the frozen ground and the release of large amounts of greenhouse gases with much higher forcing potentials. In summary, this study adds to the growing body of work suggesting that surface albedo changes need to be integrated into carbon and climate management decisions and provides related quantitative information for Eastern Siberian boreal forests.

Acknowledgments
We thank Noel Gorelick and Simon Ilyushchenko for their Google Earth Engine support. We thank Jin-Soo Kim who provided temperature and burned area trend data. Further, we thank Trofim Maximov and Alexander Isaev of the North-Eastern Federal University in Yakutsk for their help in the field and local insights. We thank Alexander Kononov for showing areas with old fire scares in the field. Further, we thank Julia Boike and Moritz Langer for their support and proof-reading. The comments of two anonymous reviewers greatly improved the manuscript. The contribution by G. S.-S. was supported by the University of Zurich Research Priority Programme on Global Change and Biodiversity. The authors declare no conflict of interest. A sample Google Earth Engine code can be found online (https://code.earthengine.google.com/d26eaeb9277c0f1c439185107e569828). Radiation data were acquired through the AsiaFlux network and are freely available upon request (http://asiaflux.net/index.php?page_id=121).

References

Achard, F., Mollicone, D., Stibig, H. J., Aksenov, D., Laestadius, L., Li, Z., et al. (2006). Areas of rapid forest-cover change in boreal Eurasia. *Forest Ecology and Management*, *237*(1–3), 322–334. https://doi.org/10.1016/j.foreco.2006.09.080

AsiaFlux. (2017). Yakutsk Spasskaya Pad larch forest data (Site Code: YLF). Retrieved April 12, 2017, from http://asiaflux.net/index.php?page_id=121

Bala, G., Caldeira, K., Wickett, M., Phillips, T. J., Lobell, D. B., Delire, C., & Mirin, A. (2007). Combined climate and carbon-cycle effects of large-scale deforestation. *Proceedings of the National Academy of Sciences of the United States of America*, *104*(16), 6550–6555. https://doi.org/10.1073/pnas.0608998104

Baldocchi, D. D., Xu, L., & Kiang, N. (2004). How plant functional-type, weather, seasonal drought, and soil physical properties alter water and energy fluxes of an oak–grass savanna and an annual grassland. *Agricultural and Forest Meteorology*, *123*(123), 13–39. https://doi.org/10.1016/j.agrformet.2003.11.006

Bathiany, S., Claussen, M., Brovkin, V., Raddatz, T., & Gayler, V. (2010). Combined biogeophysical and biogeochemical effects of large-scale forest cover changes in the MPI earth system model. *Biogeosciences*, *7*, 1383–1399. https://doi.org/10.5194/bg-7-1383-2010

Beer, C., Lucht, W., Gerten, D., Thonicke, K., & Schmullius, C. (2007). Effects of soil freezing and thawing on vegetation carbon density in Siberia: A modeling analysis with the Lund-Potsdam-Jena Dynamic Global Vegetation Model (LPJ-DGVM). *Global Biochemical Cycles*, *21*. https://doi.org/10.1029/2006GB002760

Betts, R. A. (2000). Offset of the potential carbon sink from boreal forestation by decreases in surface albedo. *Nature*, *408*(6809), 187–190. https://doi.org/10.1038/35041545

Boike, J., Grau, T., Heim, B., Günther, F., Langer, M., Muster, S., et al. (2016). Satellite-derived changes in the permafrost landscape of central Yakutia, 2000-2011: Wetting, drying, and fires. *Global and Planetary Change*, *139*, 116–127. https://doi.org/10.1016/j.gloplacha.2016.01.001

Bonan, G. B. (2008). Forests and climate change: Forcings, feedbacks, and the climate benefits of forests. *Science*, *320*(5882), 1444–1449. https://doi.org/10.1126/science.1155121

Bonan, G. B., Chapin, F. S., & Thompson, S. L. (1995). Boreal forest and tundra ecosystems as components of the climate system. *Climatic Change*, *29*(2), 145–167. https://doi.org/10.1007/BF01094014

Bonan, G. B., Pollard, D., & Thompson, S. L. (1992). Effects of boreal forest vegetation on global climate. *Nature*, *359*(6397), 716–718. https://doi.org/10.1038/359716a0

Brandt, J. P., Flannigan, M. D., Maynard, D. G., Thompson, I. D., & Volney, W. J. A. (2013). An introduction to Canada's boreal zone: Ecosystem processes, health, sustainability, and environmental issues. *Environmental Reviews*, *21*(4), 207–226. https://doi.org/10.1139/er-2013-0040

Brown, J., Ferrians Jr., O. J., Heginbottom, J. A., & Melnikov, E. S. (2002). Circum-Arctic map of permafrost and ground-ice conditions, Version 2. Boulder, CO. https://doi.org/10.3133/cp45

Chapin, F. S., Matson, P. A., & Vitousek, P. M. (2011). Earth's climate system. In *Principles of Terrestrial Ecosystem Ecology*. (pp. 23–62). New York, NY: Springer. https://doi.org/10.1007/978-1-4419-9504-9_2

Chen, D., & Loboda, T. V. (2018). Surface forcing of non-stand-replacing fires in Siberian larch forests. *Environmental Research Letters*, *13*(4), 2002–2011. https://doi.org/10.1088/1748-9326/aab443

Chen, D., Loboda, T. V., He, T., Zhang, Y., & Liang, S. (2018). Strong cooling induced by stand-replacing fires through albedo in Siberian larch forests. *Scientific Reports*, *8*(1), 1, 4821–10. https://doi.org/10.1038/s41598-018-23253-1

Chen, D., Loboda, T. V., Krylov, A., & Potapov, P. V. (2016). Mapping stand age dynamics of the Siberian larch forests from recent Landsat observations. *Remote Sensing of Environment*, *187*, 320–331. https://doi.org/10.1016/j.rse.2016.10.033

Chu, T., Guo, X., & Takeda, K. (2017). Effects of Burn Severity and Environmental Conditions on Post-Fire Regeneration in Siberian Larch Forest. *Forests*, *8*(3), 76. http://doi.org/10.3390/f8030076

De Groot, W. J., Flannigan, M. D., & Cantin, A. S. (2013). Climate change impacts on future boreal fire regimes. *Forest Ecology and Management*, *294*, 35–44. https://doi.org/10.1016/j.foreco.2012.09.027

Dickinson, E., Henderson-Sellers, A., & Kennedy, J. (1993). Biosphere-atmosphere Transfer Scheme (BATS) Version 1e as coupled to the NCAR Community Climate Model. NCAR Tech. Rep. NCAR/TN-3871STR, 72, (August), 77. https://doi.org/10.5065/D67W6959

Duveiller, G., Hooker, J., & Cescatti, A. (2018). The mark of vegetation change on Earth's surface energy balance. *Nature Communications*, *9*(1), 679. https://doi.org/10.1038/s41467-017-02810-8

ESRI (2011). *ArcGIS Desktop: Release 10*. Redlands, CA: Environmental Systems Research Institute.

Forkel, M., Thonicke, K., Beer, C., Cramer, W., Bartalev, S., & Schmullius, C. (2012). Extreme fire events are related to previous-year surface moisture conditions in permafrost-underlain larch forests of Siberia. *Environmental Research Letters*, *7*(4). https://doi.org/10.1088/1748-9326/7/4/044021

Gauthier, S., Bernier, P., Kuuluvainen, T., Shvidenko, A. Z., & Schepaschenko, D. G. (2015). Boreal forest health and global change. *Science*, *349*(6250), 819–822. https://doi.org/10.1126/science.aaa9092

Giglio, L., Descloitres, J., Justice, C. O., & Kaufman, Y. J. (2003). An enhanced contextual fire detection algorithm for MODIS. *Remote Sensing of Environment*, *87*, 273–282. https://doi.org/10.1016/S0034-4257(03)00184-6

Gorelick, N., Hancher, M., Dixon, M., Ilyushchenko, S., Thau, D., & Moore, R. (2017). Google Earth Engine: Planetary-scale geospatial analysis for everyone. *Remote Sensing of Environment*. https://doi.org/10.1016/j.rse.2017.06.031

Hansen, J., Lacis, A., Ruedy, R., Sato, M., & Wilson, H. (1993). How sensitive is the world's climate. *National Geographical Society Committee for Research and Exploration*, *9*, 142–158. Retrieved from. https://pubs.giss.nasa.gov/docs/1993/1993_Hansen_ha02800o.pdf

Hansen, J., Sato, M., & Ruedy, R. (1997). Radiative forcing and climate response. *Journal of Geophysical Research*, *102*(D6), 6831–6864. https://doi.org/10.1029/96JD03436

Hansen, M. C., Potapov, P. V., Moore, R., Hancher, M., Turubanova, S. A., Tyukavina, A., et al. (2013). High-resolution global maps of 21st-century forest cover change. *Science*, *342*(27), 850–853. https://doi.org/10.1126/science.1239552

Harris, I., Jones, P. D., Osborn, T. J., & Lister, D. H. (2014). Updated high-resolution grids of monthly climatic observations - the CRU TS3.10 dataset. *International Journal of Climatology*, *34*(3), 623–642. https://doi.org/10.1002/joc.3711

Hayasaka, H. (2002). Forest fires and climate in Alaska and Sakha Forest fires near Yakutsk. Retrieved from https://www.researchgate.net/publication/237559865_Forest_Fires_and_Climate_in_Alaska_and_Sakha_Forest_Fires_Near_Yakutsk

Hollinger, D. Y., Ollinger, S. V., Richardson, A. D., Meyers, T. P., Dail, D. B., Martin, M. E., et al. (2010). Albedo estimates for land surface models and support for a new paradigm based on foliage nitrogen concentration. *Global Change Biology*, *16*(2), 696–710. https://doi.org/10.1111/j.1365-2486.2009.02028.x

Hovi, A., Liang, J., Korhonen, L., Kobayashi, H., & Rautiainen, M. (2016). Quantifying the missing link between forest albedo and productivity in the boreal zone. *Biogeosciences*, *13*, 6015–6030. http://doi.org/10.5194/bg-13-6015-2016

IPCC. (2014). IPCC: Climate Change 2014 Synthesis Report. Contribution of Working Groups I, II and III to the Fifth Assessment Report of the Intergovernmental Panel on Climate Change. (R. K. Pachauri, L. Meyer, J.-P. Van Ypersele, S. Brinkman, L. Van Kesteren, N. Leprince-Ringuet, & F. Van Boxmeer, Eds.). Geneva, Switzerland: IPCC. Retrieved from http://ar5-syr.ipcc.ch/ipcc/ipcc/resources/pdf/IPCC_SynthesisReport.pdf

Ivanova, G. A. (1996). The extreme fire season in the central Taiga forests of Yakutia. In J. G. Goldammer, & V. V. Furyaev (Eds.), *Fire in Ecosystems of Boreal Eurasia. Forestry Sciences, Vol 48*. (pp. 260–270). Dordrecht: Springer. https://doi.org/10.1007/978-94-015-8737-2_21

Jiao, T., Williams, C. A., Ghimire, B., Masek, J., Gao, F., & Schaaf, C. (2017). Global climate forcing from albedo change caused by large-scale deforestation and reforestation: Quantification and attribution of geographic variation. *Climatic Change*, *142*(3-4), 463–476. https://doi.org/10.1007/s10584-017-1962-8

Kharuk, V., Dvinskaya, M. L., Ranson, K. J., & Im, S. T. (2005). Expansion of Evergreen conifers to the larch-dominated zone and climatic trends. *Russian Journal of Ecology*, *36*(3), 164–170. https://doi.org/10.1007/s11184-005-0055-5

Kharuk, V., Ranson, K. J., & Dvinskaya, M. L. (2007). Evidence of evergreen conifer invasion into larch dominated forests during recent decades in central Siberia. *Eurasian Journal of Forest Research*, *10*(2), 163–171. https://doi.org/10.1007/978-90-481-8641-9

Kuusinen, N., Lukeš, P., Stenberg, P., Levula, J., Nikinmaa, E., & Berninger, F. (2014). Measured and modelled albedos in Finnish boreal forest stands of different species, structure and understory. *Ecological Modelling*, *284*, 10–18. https://doi.org/10.1016/j.ecolmodel.2014.04.007

Li, Y., Zhao, M., Motesharrei, S., Mu, Q., Kalnay, E., & Li, S. (2015). Local cooling and warming effects of forests based on satellite observations. *Nature Communications*, *6*, 1–8. https://doi.org/10.1038/ncomms7603

Liu, Y., Wang, Z., Sun, Q., Erb, A. M., Li, Z., Schaaf, C. B., et al. (2017). Evaluation of the VIIRS BRDF, albedo and NBAR products suite and an assessment of continuity with the long term MODIS record. *Remote Sensing of Environment*, *201*, 256–274. https://doi.org/10.1016/j.rse.2017.09.020

Liu, Z., Ballantyne, A. P., & Cooper, L. A. (2019). Biophysical feedback of global forest fires on surface temperature. *Nature Communications*, *10*(1), 1, 214–9. https://doi.org/10.1038/s41467-018-08237-z

Lyons, E. A., Jin, Y., & Randerson, J. T. (2008). Changes in surface albedo after fire in boreal forest ecosystems of interior Alaska assessed using MODIS satellite observations. *Journal of Geophysical Research*, *113*, G02012. https://doi.org/10.1029/2007JG000606

Maximov, T. (2015). Spasskaya Pad Scientific Research Station, Station Information. Retrieved April 12, 2017, from https://eu-interact.org/field-sites/spasskaya-pad-scientific-forest-station/

Myhre, G., Shindell, D., Bréon, F.-M., Collins, W., Fuglestvedt, J., Huang, J., et al. (2013). Anthropogenic and natural radiative forcing. In T. F. Stocker, D. Qin, G. K. Plattner, M. Tignor, A. S. K. J. Boschung, et al. (Eds.), *Climate Change 2013: The physical Science Basis. Contribution of Working Group I to the Fifth Assessment Report of the Intergovernmental Panel on Climate Change* (Chap. 8). Cambridge,

Unites Kingdom and New York, NY, USA: Cambridge University Press. Retrieved from https://www.ipcc.ch/pdf/assessment-report/ar5/wg1/WG1AR5_Chapter08_FINAL.pdf

O'Halloran, T. L., Law, B. E., Goulden, M. L., Wang, Z., Barr, J. G., Schaaf, C., Brown, M., Fuentes, J. D., Göckede, M., Black, A., & Engel, V. (2011). Radiative forcing of natural forest disturbances. *Global Change Biology*, *18*(2), 555–565. https://doi.org/10.1111/j.1365-2486.2011.02577.x

Ohta, T., Hiyama, T., Tanaka, H., Kuwada, T., Maximov, T. C., Ohata, T., & Fukushima, Y. (2001). Seasonal variation in the energy and water exchanges above and below a larch forest in eastern Siberia. *Hydrological Processes*, *15*(8), 1459–1476. https://doi.org/10.1002/hyp.219

Otoda, T., Doi, T., Sakamoto, K., Hirobe, M., Nachin, B., & Yoshikawa, K. (2013). Frequent fires may alter the future composition of the boreal forest in northern Mongolia. *Journal of Forest Research*, *18*(3), 246–255. https://doi.org/10.1007/s10310-012-0345-2

Otterman, J., Chou, M.-D., & Arking, A. (1984). Effects of nontropical forest cover on climate. *Journal of Climate and Applied Meteorology*, *23*(5), 762–767. https://doi.org/10.1175/1520-0450(1984)023<0762:EONFCO>2.0.CO;2

Ponomarev, E., Kharuk, V., & Ranson, K. (2016). Wildfires dynamics in Siberian larch forests. *Forests*, *7*(6), 125. https://doi.org/10.3390/f7060125

R Core Team. (2016). R: A language and environment for statistical computing. Vienna, Austria: R Foundation for Statistical Computing. Retrieved from https://www.r-project.org/

Randerson, J. T., Chen, Y., Van Der Werf, G. R., Rogers, B. M., & Morton, D. C. (2012). Global burned area and biomass burning emissions from small fires. *Journal of Geophysical Research*, *117*, G04012. https://doi.org/10.1029/2012JG002128

Randerson, J. T., Liu, H., Flanner, M. G., Chambers, S. D., Jin, Y., Hess, P. G., et al. (2006). The impact of boreal forest fire on climate warming. *Science*, *314*. Retrieved from. https://doi.org/10.1126/science.1132075

Rogers, B. M., Soja, A. J., Goulden, M. L., & Randerson, J. T. (2015). Influence of tree species on continental differences in boreal fires and climate feedbacks. *Nature Geoscience*, *8*(3), 228–234. https://doi.org/10.1038/ngeo2352

Schaaf, C. B., & Wang, Z. (2015). MCD43A3 MODIS/Terra+Aqua BRDF/Albedo Daily L3 Global - 500m V006 [Data Set]. NASA EOSDIS Land Processes DAAC. https://doi.org/10.5067/MODIS/MCD43A4.006

Shuman, J. K., Shugart, H. H., & O'Halloran, T. L. (2011). Sensitivity of Siberian larch forests to climate change. *Global Change Biology*, *17*(7), 2370–2384. https://doi.org/10.1111/j.1365-2486.2011.02417.x

Shvidenko, A. Z., & Nilsson, S. (2000). Extent, distribution, and ecological role of fire in Russian forests. In E. S. Kasischke, & B. J. Stocks (Eds.), *Fire, Climate Change and Carbon Cycling in the Boreal Forest*. (1st ed.pp. 132–150). New York, NY, USA: Springer. https://doi.org/10.1007/978-0-387-21629-4_8

Snyder, P. K., Delire, C., & Foley, J. A. (2004). Evaluating the influence of different vegetation biomes on the global climate. *Climate Dynamics*, *23*(3–4), 279–302. https://doi.org/10.1007/s00382-004-0430-0

Takahashi, K. (2006). Future perspective of forest management in a Siberian permafrost area. Symptom of Environmental Change in Siberian Permafrost, 163–170. Retrieved from http://www.agr.hokudai.ac.jp/env/ctc_siberia/pdf_book/18_Takahashi.pdf

Tchebakova, N. M., Parfenova, E., & Soja, A. J. (2009). The effects of climate, permafrost and fire on vegetation change in Siberia in a changing climate. *Environmental Research Letters*, *4*(4), 045013. https://doi.org/10.1088/1748-9326/4/4/045013

Thomas, G., & Rowntree, P. R. (1992). The boreal forests and climate. *Quarterly Journal of the Royal Meteorological Society*, *118*(505), 469–497. https://doi.org/10.1002/qj.49711850505

Valendik, E. N. (1996). Ecological aspects of forest fires in Siberia. *Siberian Ecological Journal*, *1*, 1–18.

Wang, Z., Schaaf, C. B., Strahler, A. H., Chopping, M. J., Román, M. O., Shuai, Y., et al. (2014). Evaluation of MODIS albedo product (MCD43A) over grassland, agriculture and forest surface types during dormant and snow-covered periods. *Remote Sensing of Environment*, *140*, 60–77. https://doi.org/10.1016/j.rse.2013.08.025

Yoshikawa, K., Bolton, W. R., Romanovsky, V. E., Fukuda, M., & Hinzman, L. D. (2002). Impacts of wildfire on the permafrost in the boreal forests of interior Alaska. *Journal of Geophysical Research*, *108*(D1), 8148. https://doi.org/10.1029/2001JD000438